High Torque Double–Stator Switched Reluctance Machine for Electric Vehicle Propulsion

M. Abbasian[1], B. Fahimi[2], *Senior Member, IEEE* and M. Moallem[1], *Senior Member, IEEE*
[1]Isfahan University of Technology, Isfahan, IRAN
[2]University of Texas at Arlington, Arlington, TX 76019 USA
a_abbasian@ec.iut.ac.ir

***Abstract*-In this paper a high torque double-stator switched reluctance machine (DSSRM) is proposed for electric vehicle propulsion. DSSRM is a novel variable reluctance synchronous machine with two stators and one rotor. The magneto-motive force (mmf) orientation of these coils in DSSRM is such that a short flux path is created. To compare torque per mass of a DSSRM with that of a conventional SRM, finite element models are constructed. An experimental prototype of the proposed machine is developed and the static torque is measured. The results of our investigations indicate that the proposed geometry offers superior performance in terms of higher torque per mass.**

I. INTRODUCTION

There is a growing interest in electric vehicle (EV) due to air pollution and exhaustion of fossil fuels. Induction motors and permanent magnet synchronous motors are commonly used to obtain the driving force in EVs [1]. There are, however, several disadvantages of these motors, such as control complexity and manufacturing costs, etc. Switched reluctance motors (SRMs) have a simple construction and high reliability [2]. In addition, SRMs are low cost because SRMs do not have permanent magnets. These features satisfy the requirements of the EVs [3].

The first design of this motor for EV applications was reported in [4], where an SRM was designed for higher efficiency operation. Test results showed superior operation and higher power density of SR motor when compared to an induction motor.

Nevertheless, SRMs had been only used in starter motor of the airplane or the fuel pump due to the disadvantages, such as the acoustic noise and the torque ripple [4]. Recently, the development of power electronics enables to reduce these disadvantages, and it has been considered for application to EV and other kind of electrical apparatuses.

The traction drive needs the large torque under low speed region to overcome the starting friction and wide constant power region.

Fast acceleration and deceleration can be realized with low high torque per mass of the machine. In the case of the EV, the machine design to satisfy that requirement is the first work to be done.

Alternate designs of SRM with high torque density have been introduced by some researchers. In [5] a low-cost and energy-efficient SR motor for EV application is designed and built. [6] presented an SR prototype for a hybrid vehicle starter/alternator application. In [7]-[8] Xu and Lipo explored the utilization of axially laminated rotor structures for SRMs. A patent by Horst [9] concerning the use of segmented rotor constructions for unidirectional operation of two-phase SRMs is another example of this approach [10].

A review of the literature indicates that the majority of the electromagnetic forces that are generated within a conventional SRM do not contribute to the motion. In fact a significant part of these forces will initiate undesirable vibrations that have been identified as a major drawback for SRM drives. The goal of the present article is to introduce an alternative geometry using which a greater percentage of the electromagnetic forces will contribute to the motion (i.e. motional forces).

In order to accomplish this goal, an alternative double-stator switched reluctance machine (DSSRM) is introduced. Using finite element analysis the performance of the proposed geometry and that of a conventional SRM from a torque density point of view will be compared.

II. ELECTROMAGNETIC ENERGY CONVERSION PROCESS IN SRM

The electromagnetic forces within an electric machine can be viewed as the product of interaction between normal and tangential components of the flux density. These flux densities can be originated by electromagnets, permanent magnets, or polarized ferromagnetic materials.

In SRM magnetic force production is highest where the highest reluctance variation occurs (viz. along the edges of the moving iron). The relative amplitude of force components are determined based on the same concept, i.e. the more energy change in a given direction, the higher the force component at that direction. Since the magnetic field intensity and magnetic energy are very small in unsaturated ferromagnetic material, the force contributions from these regions are negligible as compared to the airgap. If the ferromagnetic material is considered as an incompressible material having very high permeability compared to air, then the volume force density inside iron is very small and the magnetic force density reduces to the surface force density acting on the surface of the iron. This surface force density can also be expressed using Maxwell Stress Tensor (MST) method. The normal and tangential components of the force density in the airgap are given by :

$$f_n = \frac{1}{2\mu_0}(B_n^2 - B_t^2) \quad (1)$$

978-1-4244-8218-4/10/$26.00 ©2010 IEEE

$$f_t = \frac{1}{\mu_0}(B_n B_t) \quad (2)$$

where f_n, f_t, B_n, B_t and μ_0 denote the normal component of the force density, the tangential component of the force density, the normal component of the flux density, the tangential component of the flux density and absolute permeability, respectively.

At the two dimensional cross section of an electromagnetic motion device, there are two field components and two force components which are related with each other by various formulations given by Lorentz law, Maxwell Stress Tensor method, and Virtual Work method. In all formulations, the normal force distribution is a function of square of field components and tangential force distribution is function of their products. At the iron-air interface, and in the absence of a surface current density (viz. SRM), the continuity theorem suggests,

$$B_{n,iron} = B_{n,air} \quad (3)$$

$$H_{t,iron} = H_{t,air} \quad (4)$$

Within a ferromagnetic material with high relative permeability ($\mu_{r,iron}$), the field intensity and its normal and tangential components ($H_{n,iron}, H_{t,iron}$) are very small. Therefore, both the tangential and normal components of the force inside iron ($f_{n,iron}, f_{t,iron}$) and at the iron-side of interface are close to zero. Investigation of the field components at the interface using (3) and (4) indicates that the tangential component of the flux density in the airside of the interface ($B_{t,air}$) is significantly smaller than the normal component ($B_{n,air}$). This observation suggests that most flux lines in the air-side of the interface are perpendicular to the surface of the iron.

$$B_{n,air} = B_{n,iron} \quad (5)$$

$$B_{t,air} = \frac{1}{\mu_{r,iron}} B_{t,iron} \quad (6)$$

Thus at the air-side of the interface, the tangential component of the force density ($f_{t,air}$) is almost zero. However, one may note that there exists a very large normal component of the force on the air-side of the interface ($f_{n,air}$) between iron and air. This can be explained by the following expressions:

$$f_{n,air} = \frac{1}{2\mu_0}(B_{n,air}^2 - B_{t,air}^2) \approx \frac{1}{2\mu_0} B_{n,air}^2 \quad (7)$$

$$f_{t,air} = \frac{1}{\mu_0}(B_{n,air}.B_{t,air}) \approx \frac{1}{\mu_0 \mu_r} B_{n,air}.B_{t,iron} << f_{n,air} \quad (8)$$

Therefore, one can say that the forces on a current-free iron are produced on the surface of iron as the normal force component which is directed toward the air [8]. These forces are stronger where the surface flux density is higher. If this normal force happens to be in the direction of motion it is viewed as a useful result of the electromechanical energy conversion. Otherwise it is viewed as a troublesome by-product that causes noise, vibration, and deformation. The higher the normal surface force in the direction of movement and lower on other directions, the more efficient energy conversion process becomes. In SRM, the motional forces are much less than non-motional forces which means that a small part of magnetic energy of the field is converted to useful mechanical work (viz. the efficiency of the energy conversion process is low.

III. DOUBLE-STATOR SWITCHED RELUCTANCE MACHINE

A. Configuration of the Machine

The proposed SRM, double-stator switched reluctance machine (DSSRM), is a variable reluctance synchronous machine that is designed to produce high torque density. Fig. 1 and Fig. 2 show the configuration of the DSSRM. In this machine two stators are employed. These stators are made of laminated ferromagnetic material (M-19) and are equipped with concentrated windings. The two stators are located on the interior and exterior of a cylindrical rotor. The rotor is formed by segments of laminated M-19 which is hold together using a non-ferromagnetic cage. In the proposed 8:6 DSSRM, the number of stator and rotor poles (segments) is 8 and 6 respectively.

The operational principle of DSSRM is similar to that of conventional SRM. In DSSRM, under motoring mode of operation, the electromagnetic torque is generated by the tendency of the magnetic circuit to minimize the reluctance. The relative position between rotor and stator (θ) has been illustrated in Fig. 3, when rotor is at aligned position ($\theta = 0$). If the rotor is at unaligned position, the rotor tends to move; thereby minimizing the reluctance of the system and achieving the shortest flux path in the air. Continuing with the sequence of the stator phases, one can notice that similar to a conventional SRM, a counterclockwise excitation pattern among stator phases will result in a clockwise motion and visa verse.

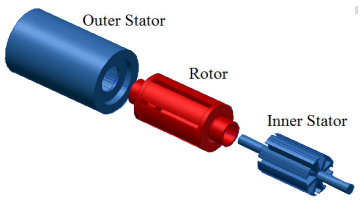

Fig. 1. Stators and rotor of the DSSRM

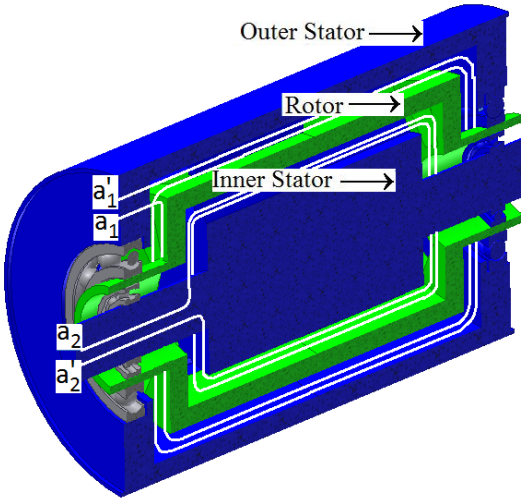

Fig. 2. Configuration of the DSSRM

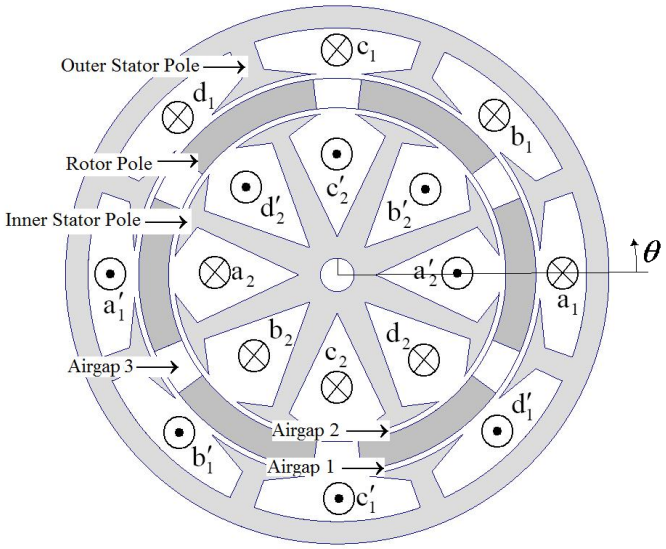

Fig. 3. Cross section of a 4-phase DSSRM.

B. Finite Element Analysis

In order to investigate the flux path of DSSRM, a two dimensional finite element model of the DSSRM prototype (see Fig. 6) with the parameters presented in Table I is constructed. The finite element model is solved when the current of phase "a" is set to 20 A. Three critical positions are chosen: unaligned position ($\theta = 30^o$), half-aligned position ($\theta = 15^o$) and aligned position ($\theta = 0^o$). Fig. 4 illustrates the flux patterns at these three positions when rotor moves in clockwise direction.

Based on the finite element analysis of the DSSRM, the static torque profiles of the DSSRM at various rotor positions for $i_a = 2.5A$ to $i_a = 20A$ are calculated and illustrated in Fig. 5. In order to compare the torque density of the DSSRM with conventional SRM, the static torque of a conventional 8/6 SRM for $i_a = 20A$ is also calculated and shown in Fig 5. The parameters of the conventional SRM are presented in Table II. Although a one to one correspondence between all design parameters of the two topologies (DSSRM and conventional SRM) is impossible, care has been given to maintain the same stack length, same outer diameter, same wire gauge and phase current amplitude, and same overall mass (copper and iron combined). The individual airgap length in the radial direction separating the stator/s and rotor is kept at 1 mm on both sides. The results shown in Fig. 5 confirm that using the new topology, better Torque density is achieved. It can be observed that the 8/6 prototype DSSRM produces 300% higher peak torque than the conventional SRM.

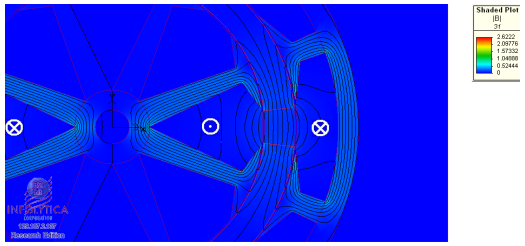

(a)

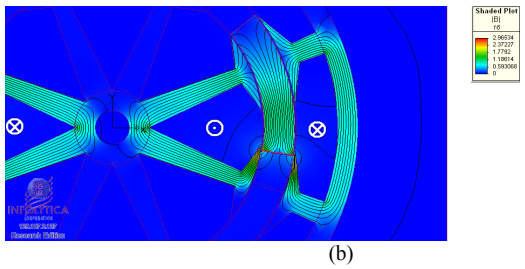

(b)

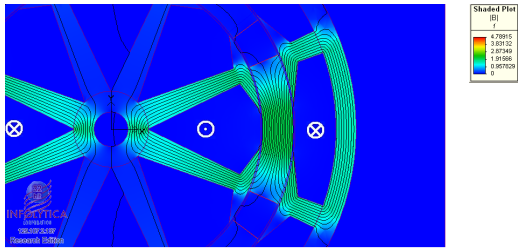

(c)

Fig. 4. Flux plot at three rotor positions: (a) unaligned position, $\theta = 30^o$, (b) half-aligned position, $\theta = 15^o$, (c) aligned position, $\theta = 0^o$

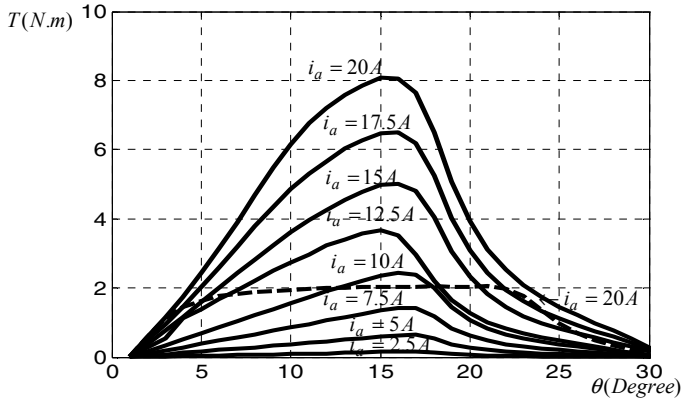

Fig. 5. Torque of DSSRM at various rotor positions for $i_a = 2.5A$ to $i_a = 20A$ (solid line) along with torque of the conventional SRM for $i_a = 20A$ (dashed line)

IV. Experimental Results

The static torque measurement is made in this study using a experimental setup as shown in Fig. 7. To perform the test, rotor is locked in each specific rotor position using the index head. A torque meter is installed between rotor shaft and index head. A dc current is injected to the phase winding. The output voltage of the torque meter is measured and the static torque for different rotor positions and currents are obtained. Fig. 8 shows the measured static torque of DSSRM compared with the calculated static torque using Finite element analysis.

Fig. 6. The experimental prototype of the DSSRM

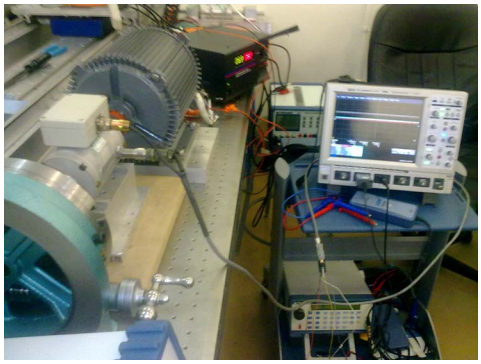

Fig. 7 The test set-up for static torque measurement.

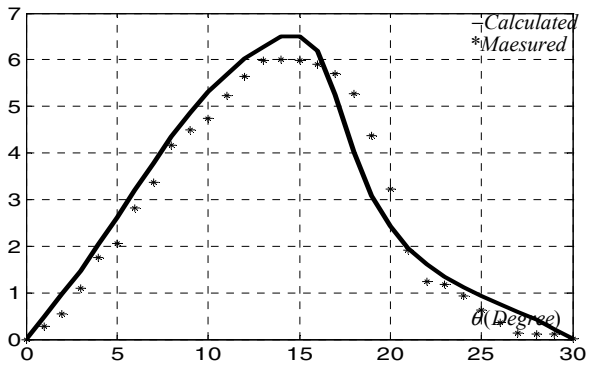

Fig. 8. Torque of DSSRM at various rotor positions for $i_a = 17.5A$

TABLE I
PARAMETERS OF THE DSSRM

Number of stator poles	8
Number of rotor poles(Segments)	6
Number of phases	4
Outer radius of outer stator	72.0mm
Outer radius of inner stator	43.9mm
Rotor segment thickness	9.0 mm
Airgap 1 and Airgap 2	1.0mm
Stack length	115.0mm
Arc of the rotor segments	47 degree
Number of turns per phase	50
Rated current	30A
Rated voltage	100V
Resistance per phase	0.78 Ω
Stator winding material	copper
Lamination material	M19
Mass of copper	3.1kg
Mass of iron	5.0kg

TABLE II
PARAMETERS OF THE SRM

Number of stator poles	8
Number of rotor poles	6
Number of phases	4
Outer radius of stator	72.0mm
Outer radius of rotor	38.3mm
Airgap	1.0mm
Stack length	115.0mm
Number of turns per phase	32
Rated current	30A
Rated voltage	100V
Stator winding material	copper
Lamination material	M19
Mass of copper	1.8kg
Mass of iron	6.3kg

V. Conclusions

A new double stator switched reluctance machine (DSSRM) is introduced for electric vehicle applications. Unlike conventional SRM in which majority of the electromagnetic force are applied in radial direction (hence not contributing to the motion), DSSRM offers a much more efficient configuration in terms of generation of motional forces In DSSRM, by the virtue of engineering a novel flux path, a substantial improvement in torque density is accomplished. Through a comparison, it has been demonstrated that the proposed DSSRM exhibit superior performance indices as compared to conventional SRM and as such is viewed as a serious contender for electric vehicle propulsion.

References

[1] X. D. Xue, K. W. E. Cheng, J. K. Lin, Z. Zhang, K. F. Luk, T. W. Ng, and N. C. Cheung,” Optimal Control Method of Motoring Operation for SRM Drives in Electric Vehicles”, *IEEE Trans. Vehic. Tech.*, vol. 59, no. 3, pp 1191-1199, Mar 2010.

[2] T. J. E. Miller, *Electronic Control of Switched Reluctance Machines*. New York: Reed Educational and Professional, 2001, pp. 227–245.

[3] Khwaja M. Rahman, and Steven E. Schulz,” Design of High-Efficiency and High-Torque-Density Switched Reluctance Motor for Vehicle Propulsion”, IEEE TRANSACTIONS ON INDUSTRY APPLICATIONS, VOL. 38, NO. 6, NOVEMBER/DECEMBER 2002.

[4] P. J. Blake, R. M. Davis, W. F. Ray, N. N. Fulton, P. J. Lawrenson, and J. M. Stefenson, "The control of switched reluctance motors for battery electric road vehicles," in *Proc. Int. Conf. PEVD*, May 1984, pp. 361–364.

[5] H. Lang and F. J.Vallese, "Variable reluctance motor drives for electric propulsion," U.S. Dept. Energy, Washington, DC, DOE/CS-54209–26, 1985.

[6] J. M. Miller, A. R. Gale, P. J. McCleer, F. Leonardi, and J. H. Lang, "Starter-alternator for hybrid electric vehicles: Comparison of induction and variable reluctance motors and drives," in *Conf. Rec. IEEE-IAS Annu. Meeting*, vol. 1, 1998, pp. 513–523.

[7] L. Xu, "Design and evaluation of a converter optimized synchronous reluctance motor drive," Ph.D. dissertation, Univ. Wisconsin-Madison, Madison, WI, 1990.

[8] T. A. Lipo and L. Xu, "Variable Speed Machine with High Power Density," U.S. Patent no. 5 010 267, April 23, 1991.

[9] G. A. Horst, "Isolated Segmental Switched Reluctance Motor," U.S. Patent no. 5 111 096, May 5, 1992.

[10] B. C. Mecrow, E. A. El-Kharashi, J. W. Finch and Alan G. Jack," Preliminary Performance Evaluation of Switched Reluctance Motors with Segmental Rotors," *IEEE Transactions on Energy Conversion*, vol. 19, no. 4, pp. 679- 686, Dec. 2004.